NATURAL CONVECTION IN TWO DIFFERENT ENCLOSURES FILLED WITH NANOHYBRID UNDER MAGNETIC FIELD: APPLICATION TO HEAT EXCHANGER

Raouia AZZOUZ[1], Mohamed Bechir BEN HAMIDA[*2,1,3]

[1]Research Laboratory of Ionized Backgrounds and Reagents Studies (EMIR), Preparatory Institute for Engineering Studies of Monastir (IPEIM), University of Monastir, Monastir City, Tunisia.

[2]College of Engineering, Department of Chemical Engineering, Imam Mohammad Ibn Saud Islamic University (IMSIU), Riyadh, Saudi Arabia.

[3]Higher School of Sciences and Technology of Hammam Sousse (ESSTHS), University of Sousse, Sousse City, Tunisia.

[*] Corresponding author: MBHamida@imamu.edu.sa/benhamida_mbechir@yahoo.fr

The current numerical work examines the thermal energy transport controlled by magnetohydrodynamic buoyancy inside two distinct enclosure shapes filled with water-Ag-MgO nanohybrids. The outer wall of the enclosure is designed to be frigid, but the inner spaces are heated continuously. To do this, we used Comsol Multiphysics to develop a two-dimensional code that solved the equations related mass, momentum, and energy. When the Prandtl number is assumed to be Pr = 6.58, the impact of relevant parameters such as Rayleigh number between 10^3 and 10^6, Hartmann number between 0 and 120, and the solid volume fraction of the nanohybrid on the flow and heat transfer performance of the enclosure are investigated after the validation of the numerical code. It is obtained that the average Nusselt number is a function of and increases with solid volume fraction of the nanohybrid. Furthermore, the average Nusselt number drops with Ha, with the effect being more pronounced for higher Rayleigh values.

Key words*: Hybrid nanofluids, Heat transfer, Magnetic field, Natural convection, Comsol Multiphysics.*

1. Introduction

The rate of heat transfer in equipment used in different sectors has been the subject of numerous studies in recent years, due to its prevalence in various engineering fields, such as LED lamps [1–3], plasma manufacturing [4,5], and also, the enhancement of the performance of thermal systems including solar collectors [6,7], heat exchangers [8–10], bubble absorber systems [11,12], and systems for condensing and evaporating [13]. So, in order to increase the rate of heat transfer, special geometries [8] or using enriched fluids [12], such as nanofluids, can be configured or thermal areas can be increased, also it is possible to apply an electric current or magnetic field [14–18]. Due to their better thermal properties, nanofluids have recently gained popularity as a study area. In order to improve combined heat and mass transfer in ammonia-water bubble absorption processes, binary nanofluid is used in Ben Hamida *et al.* [12] paper's in-depth analysis. A systematic study shows that

nanoparticles boost gas absorption in absorbers, allowing for potentially smaller designs, and even enhance mass and heat transfer in binary nanofluids, especially at lower flow rates, lower starting concentrations, and higher temperatures [19].

A potential heat transfer medium is hybrid nanofluid, which is an extension of binary nanofluid and contains two or more different types of nanoparticles inside the base fluid. So, by adopting hybrid nanofluid as a cooled ammonia-water absorption system, bubble absorbers can perform better and shrink in size [20]. Additionally**,** Ben Jabalah *et al.* [21] was discovered that hybrid nanofluids boost ammonia-water absorption but require optimal absorber design for full effect. Safaie *et al.* [22] investigates how radiation and free convection influence heat transfer in shallow cavity nanofluids, revealing their impact on flow behavior and heat transfer mechanisms. Ben Hamida *et al.* [1] using four water-based hybrid nanofluids to cool LEDs found all fluids reduced LED temperature, with Al2O3-TiO2 performing highest Nusselt number for heat transfer. Even a small increase (0.01%) in nanoparticle concentration significantly enhanced heat transfer (5.19% locally and 0.43% on average). Due to its various engineering uses, the effect of magnetic fields in enclosures has drawn the utmost interest from researchers. A numerical analysis of natural convection in the presence of magnetic fields in a square enclosure containing an ethylene glycol-copper nanofluid was carried out [15]. Additionally, Ben Hamida *et al.* [23] explores heat transfer in a water-Ag-MgO nanohybrid fluid under a magnetic field. They found that increasing the electric field voltage from 1V to 5V significantly boosted heat transfer capability.

To solve the physical models, based on finite technical elements, we have developed a numerical study using the software COMSOL Multiphysics 6.1.

In a quest for radically improved heat transfer in cavities, essential for efficient heat exchangers, this research explores a groundbreaking two-pronged approach: geometry optimization and hybrid nanofluid integration. We compare the heat transfer capabilities of traditional circular cavities to a novel, high-performance flower-shaped design, demonstrating its potential as a game-changer in heat exchanger technology. Furthermore, we move beyond conventional single-nanoparticle fluids by investigating the synergistic effects of hybrid nanofluids, which offer significantly enhanced heat transfer. This combined approach provides valuable insights that surpass studies limited to a single factor. Future work could involve transient simulations to delve deeper into the time-dependent heat transfer dynamics within these cavities.

2. Formulation of the problem

The coordinate system and physical model are depicted in Figure 1. A circular enclosure of diameter L filled with water-Ag-MgO nanohybrid makes up the initial computational domain. Along the horizontal and vertical mid-plane, four inner circular cylinders with diameters of d are spaced apart at a distance of s. A flower-shaped enclosure with dimensions L_1 and L_2 included within it two gaps with the same outer shape in dimensions d_1 and d_2 make up the second computational domain, which is also filled with water-Ag-MgO nanohybrid. The outer walls of the two types of enclosure are set to temperature T_c, while the inner ones are set to temperature T_h. The two models were designed to be with the same area to be compared. In the vertical direction, a magnetic field of uniform strength B_0 is applied. It was determined that B_0 was a variable where Hartmann number changed from 0 to the greatest value of 120.

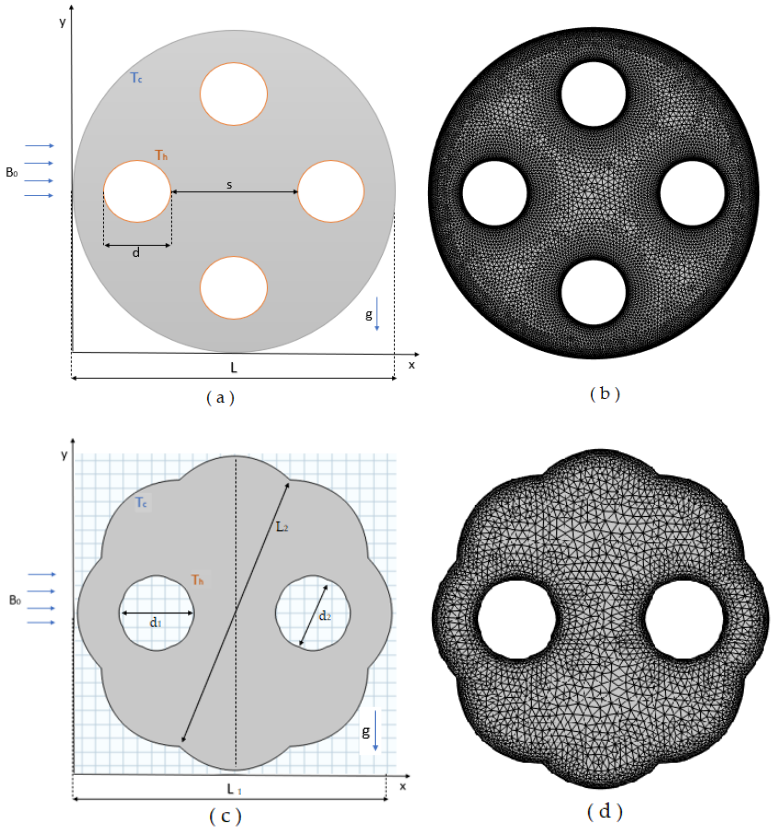

Fig. 1. (a)-Schematic of the shape 1 of the physical problem; (b) – Mesh of shape 1 used in Comsol Multiphysics
(c)-Schematic of the shape 2 of the physical problem; (d) – Mesh of shape 2 used in Comsol Multiphysics

Table 1 provides an overview of the boundary criteria applied to dimensional and dimensionless forms. The boundaries of the geometries were designated numerically. For the circular shape, '1-1' represents the outer boundary, while '1-2,' '1-3,' '1-4,' and '1-5' represent the boundaries of the four inner circles. Similarly, in the flower shape, '2-1' denotes the outer boundary, and '2-2' and '2-3' represent the inner boundaries.

Table 1. Boundary conditions.

	Dimensional form			**Dimensionless form**		
Border	Condition on u	Condition on v	Condition on T	Condition on u^*	Condition on v^*	Condition on T^*
1-1	0	0	T_c	0	0	0
1-2	0	0	T_h	0	0	1
1-3	0	0	T_h	0	0	1
1-4	0	0	T_h	0	0	1
1-5	0	0	T_h	0	0	1
2-1	0	0	T_c	0	0	0
2-2	0	0	T_h	0	0	1
2-3	0	0	T_h	0	0	1

In our study, specific temperatures are utilized along with a Prandtl number (Pr) to clearly define the hydrodynamic and thermal boundary conditions. The inner boundaries, symbolizing the heated cylinders, are persistently maintained at a temperature of Th = 1, while the outer boundaries, representing the enclosure walls, remain steady at a temperature Tc = 0. This creates a significant

temperature contrast that drives the heat transfer process. Additionally, the Prandtl number is set to $Pr = 6.58$, indicating a moderately viscous fluid where heat conduction plays a more prominent role compared to bulk fluid motion.

All dimensions are sited in table 2.

Table 2. Dimensions of the model studied.

Parameters	Values
L (m)	0.45
L_1 (m)	0.45237
L_2 (m)	0.41529
s (m)	0.18
d (m)	0.09
d_1 (m)	0.108
d_2 (m)	0.10468

2.1. Hypotheses

In this work, the following hypotheses are taken into consideration:

- It is assumed that fluid flow is laminar, steady, two-dimensional, and incompressible.
- Heat and mass are transmitted in both directions (x,y).
- The Boussinesq approximation yields constant fluid characteristics.
- The transfer of radiant heat is not considered
- Viscous dissipation's impact is disregarded.
- The approximations for the boundary layer are accurate.
- The hybrid nanofluid is treated as one liquid phase.
- The nanoparticles are uniformly dispersed.

2.2. Governing equations

Utilizing the below-presented simplifying assumptions, the bidimensional, cartesian coordinates (x, y), equation system for thermal energy, linear momentum, and continuity is used to manage our physical problem.

2.2.1 The dimensional governing equation

- *Mass conservation equation*

$$\frac{\partial u}{\partial x}+\frac{\partial v}{\partial y}=0 \tag{1}$$

- *According to x, the momentum conservation equation*

$$\rho_{hnf}\left(u\frac{\partial u}{\partial x}+v\frac{\partial u}{\partial y}\right)=-\frac{\partial p}{\partial x}+\mu_{hnf}\left(\frac{\partial^2 u}{\partial x^2}+\frac{\partial^2 u}{\partial y^2}\right) \tag{2}$$

- *According to y, the momentum conservation equation*

$$\rho_{hnf}\left(u\frac{\partial v}{\partial x}+v\frac{\partial v}{\partial y}\right)=-\frac{\partial p}{\partial y}+\mu_{hnf}\left(\frac{\partial^2 v}{\partial x^2}+\frac{\partial^2 v}{\partial y^2}\right)-vB_0^2\sigma_{hnf}+\rho_{hnf}\beta_{hnf}g(T-T_c) \tag{3}$$

- *Energy conservation equation*

$$\left(u\frac{\partial T}{\partial x}+v\frac{\partial T}{\partial y}\right)=\alpha_{hnf}\left(\frac{\partial^2 T}{\partial x^2}+\frac{\partial^2 T}{\partial y^2}\right) \quad (4)$$

2.2.2 The non-dimensional governing equation

Following the use of these numerous non-dimensional parameters and variables:

$x^*=\frac{x}{L}, y^*=\frac{y}{L}, u^*=\frac{uL}{\alpha_f}, v^*=\frac{vL}{\alpha_f}, T^*=\frac{T-T_c}{T_h-T_c}, p^*=\frac{pL^2}{\rho_{nf}\alpha_f^2}, Pr=\frac{\vartheta_f}{\alpha_f}, Ha=B_0L\sqrt{\frac{\sigma_f}{\rho_f\vartheta_f}}, Ra=\frac{g\beta_f L^3(T_h-T_c)}{\vartheta_f\alpha_f}$.

Our system of dimensionless equations is written as follows:

- *Mass conservation equation*

$$\frac{\partial u^*}{\partial x^*}+\frac{\partial v^*}{\partial y^*}=0 \quad (5)$$

where, respectively, u^* and v^* represent the dimensionless velocities corresponding to $x^*$and y^*.

- *According to x^*, the momentum conservation equation*

$$\left(u^*\frac{\partial u^*}{\partial x^*}+v^*\frac{\partial u^*}{\partial y^*}\right)=-\frac{\partial p^*}{\partial x^*}+Pr\frac{\vartheta_{hnf}}{\vartheta_f}\left(\frac{\partial^2 u^*}{\partial x^{*2}}+\frac{\partial^2 u^*}{\partial y^{*2}}\right) \quad (6)$$

- *According to y^*, the momentum conservation equation*

$$\left(u^*\frac{\partial v^*}{\partial x^*}+v^*\frac{\partial v^*}{\partial y^*}\right)=-\frac{\partial p^*}{\partial y^*}+Pr\frac{\vartheta_{hnf}}{\vartheta_f}\left(\frac{\partial^2 v^*}{\partial x^{*2}}+\frac{\partial^2 v^*}{\partial y^{*2}}\right)-v^*\frac{\sigma_{hnf}\rho_f}{\sigma_f\rho_{hnf}}Ha^2Pr+\frac{\beta_{hnf}}{\beta_f}RaPrT^* \quad (7)$$

- *Energy conservation equation*

$$\left(u^*\frac{\partial T^*}{\partial x^*}+v^*\frac{\partial T^*}{\partial y^*}\right)=\frac{\alpha_{hnf}}{\alpha_f}\left(\frac{\partial^2 T^*}{\partial x^{*2}}+\frac{\partial^2 T^*}{\partial y^{*2}}\right) \quad (8)$$

2.2.3 Hybrid nanofluid properties

The mixing theory of Ho *et al.* [24] can be used to compute the hybrid nanofluid's density as shown below.

$$\rho_{hnf}=(1-\varphi)\rho_{bf}+\varphi_{Ag}\rho_{Ag}+\varphi_{MgO}\rho_{MgO} \quad (9)$$

Where *bf* and *hnf* represent, respectively, the base fluid and the hybrid nanofluid.

The formulas below define φ as the volume fraction of two different kinds of nanoparticles.

$$\varphi=\varphi_{Ag}+\varphi_{MgO} \quad (10)$$

Where, $\varphi_{Ag}=\frac{\varphi}{2}$ and $\varphi_{MgO}=\frac{\varphi}{2}$.

The parameters of the nanofluid are ascertained using the classical models documented in the literature.[15]

$$\sigma_{hnf} = (1-\varphi)\sigma_{bf} + \varphi_{Ag}\sigma_{Ag} + \varphi_{MgO}\sigma_{MgO} \tag{11}$$

$$(\rho\beta)_{hnf} = (1-\varphi)(\rho\beta)_{bf} + \varphi_{Ag}\beta_{Ag} + \varphi_{MgO}\beta_{MgO} \tag{12}$$

$$\alpha_{hnf} = \frac{k_{hnf}}{(\rho C_p)_{hnf}} \tag{13}$$

The following equations provide the specific heat capacity of hybrid nanofluids:

$$Cp_{hnf} = \frac{(1-\varphi)\rho_{bf}Cp_{bf} + \varphi_{Ag}\rho_{Ag}Cp_{Ag} + \varphi_{MgO}\rho_{MgO}Cp_{MgO}}{\rho_{hnf}} \tag{14}$$

According to the Maxwell model [25], the hybrid nanofluid's thermal conductivity is determined as follows:

$$\frac{k_{hnf}}{k_{bf}} = \frac{\frac{(\varphi_{Ag}k_{Ag} + \varphi_{MgO}k_{MgO})}{\varphi} + 2k_{bf} + 2(\varphi_{Ag}k_{Ag} + \varphi_{MgO}k_{MgO}) - 2\varphi k_{bf}}{\frac{(\varphi_{Ag}k_{Ag} + \varphi_{MgO}k_{MgO})}{\varphi} + 2k_{bf} - (\varphi_{Ag}k_{Ag} + \varphi_{MgO}k_{MgO}) + \varphi k_{bf}} \tag{15}$$

According to Brinkman's model [26], the dynamic viscosity of a hybrid nanofluid is defined as follows:

$$\mu_{hnf} = \frac{\mu_{bf}}{(1-\varphi_{Ag}-\varphi_{MgO})^{2.5}} \tag{16}$$

Table 3 lists the hybrid nanofluid's constant thermophysical characteristics [12,27].

Table 3. Thermophysical properties of base fluid (water) with used nanoparticles

Physical properties	Ag [27]	MgO [28]	Water [27]
Density ρ (kg/m^3)	10500	3580	997.1
Specific heat Cp (J/kg K)	535.6	955	4179
Thermal conductivity *k* (W/m K)	429	45	0.613
Thermal expansion coefficient β (1/K)	0.85		21
Dynamic viscosity μ (kg/m s)	-	-	$8.91.10^4$

2.2.4 Nusselt number

The Nusselt number, a dimensionless metric, is used to represent heat transfer. The established local Nusselt number on the hot inner wall is defined as:

$$Nu_l = -\frac{k_{hnf}}{k_{bf}}\left(\frac{\partial T^*}{\partial x^*} + \frac{\partial T^*}{\partial y^*}\right) \tag{17}$$

The average Nusselt number Nu_m is calculated by integrating Nu_l:

$$Nu_m = -\frac{1}{A}\int_0^1 Nu_l \, dA \tag{18}$$

Where A is the total surface area.

3. Resolving and validating numerical code

Using the finite element-based software COMSOL Multiphysics 6.1, every system of equations used in this work that was previously described in detail, was solved. The extra-fine mesh has proven to be the best mesh after several mesh type testing in terms of a good validation of our numerical code with the experimental results. Figure 1.b. illustrates this form of mesh, which has 20024 elements and 852 boundary elements for a circular shape and 17164 elements and 704 boundary elements for the second case shape shown in Figure 1.d. The current study is corroborated by contrasting Nu for various Ha values at $Ra = 10^6$ and $\varphi = 0.05$ with the outcomes of Ben Hamida *et al.* [15] for magnetohydrodynamic natural convection in a square enclosure filled with ethylene glycol-Cu nanofluids, as shown in Table 4. The findings of the current study are in good agreement with those of Ben Hamida *et al.* [15].

Table 4. Average Nusselt number for various Ha values at $Ra = 10^6$ and $\varphi = 0.05$ on the hot bottom wall

Ha	Ben Hamida [15]	Present work			
		Normal	Fine	Finer	Extra fine
0	9.94	9.86	9.89	9.92	9.98
20	9.12	8.96	9.01	9.04	9.18
40	7.5	7.38	7.43	7.45	7.56
60	6.05	6.13	6.13	6.09	6.06
120	3.35	3.93	3.78	3.55	3.38

As can be seen from table 4, the extra-fine mesh demonstrates the closest agreement in Ha values compared to the reference study by Ben Hamida *et al.* [15]. This convergence towards the established results strengthens the validation of our numerical code and justifies our selection of the extra-fine mesh for further simulations. To ensure the accuracy and efficiency of our numerical simulations, we conducted a mesh independence study. This study involved evaluating the Nusselt number with progressively finer mesh densities. Table 5 presents the Nusselt number values obtained for various mesh types, ranging from extremely coarse to extremely fine.

As observed in the table, the Nusselt number exhibits a decreasing trend with increasing mesh density, indicating a refinement in the solution. Notably, the Nusselt numbers obtained with the 'extra fine' and 'extremely fine' meshes is the same. This suggests that the 'extra fine' mesh provides a sufficient level of discretization for capturing the flow and heat transfer phenomena with minimal mesh-induced errors. Therefore, the 'extra fine' mesh was chosen as the optimal mesh density for subsequent simulations, balancing accuracy with computational efficiency.

Table 5. Mesh Independence

Ha	Extremely coarse	Extra coarse	Coarser	Coarse	Normal	Fine	Finer	Extra fine	Extremely fine
0	3.38	3.35	3.40	3.42	3.41	3.42	3.44	3.46	3.46
20	3.35	3.32	3.37	3.39	3.38	3.39	3.41	3.43	3.43
40	3.27	3.25	3.29	3.31	3.30	3.32	3.34	3.35	3.35
60	3.18	3.16	3.21	3.23	3.22	3.23	3.25	3.27	3.27
80	3.11	3.09	3.14	3.16	3.15	3.17	3.19	3.20	3.20
100	3.06	3.05	3.09	3.11	3.11	3.12	3.14	3.16	3.16
120	3.03	3.02	3.06	3.09	3.08	3.09	3.11	3.13	3.13

4. Results and Discussions

4.1. Flow field

In terms of streamlines, the combined effects of the Hartmann number and the hybrid nanofluid volume fraction on the flow features are investigated. Figure 2 and 3 shows the streamlines at $Ra = 10^6$ in different φ values of the circular and flower shape case, respectively. It is apparent that fluid close to the heated walls warms up and flows to the extremities of the outer wall in both cases. When the fluid particles come into contact with the neighboring cool surface, they fall, forming recirculation zones. Also, the vortices seem to get stronger uniformly as they get closer to the outside wall of in the circular case shape and in the case of the flower-shaped enclosure, the fluid particles fall after coming into contact with the top, cold surface, creating recirculation zones there compared to the bottom. By adding hybrid nanofluid, the density of the vortices is increased in the two shape cases which strengthens the flow cell. Convection impact, which is more pronounced at much higher Rayleigh numbers and eventually increases the force of such vortices, is the cause of this. It is clear that when Ha increases, the intensity of the vortices decreases because the magnetic force suppresses the buoyant force.

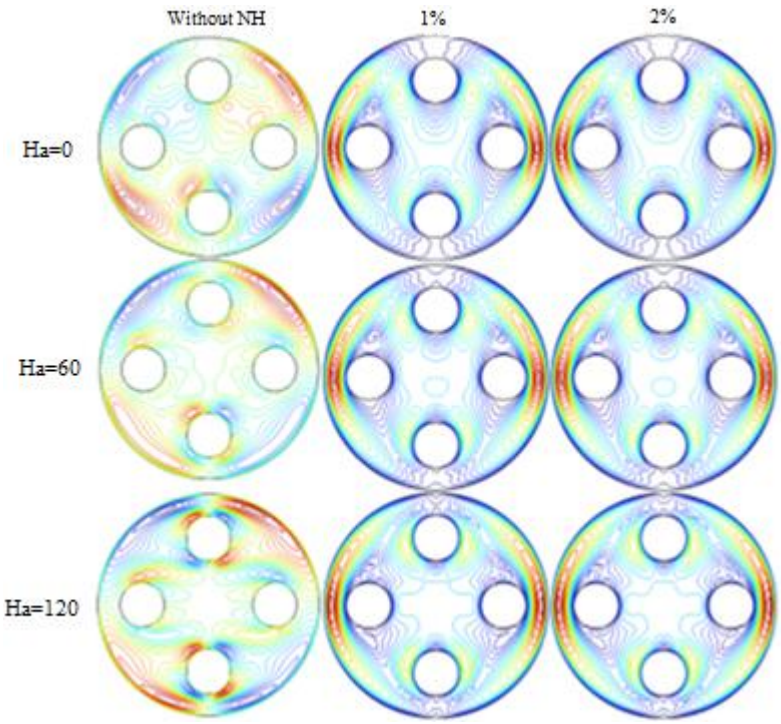

Fig. 2. Dimensionless streamlines for the circular shape at $Ra = 10^6$ in different φ values.

4.2. Temperature field

A thorough examination of isotherms helps for learning the physics involved in heat transmission within the two shapes used. Figure 4 and 5 shows, respectively, the isotherms of the circular and flower shape case at $Ra = 10^6$ in different φ values. It is clear that the convective flow becomes weaker as the magnetic field strength increases. when a result, when Ra increases, the isotherms often arrange themselves in a parallel pattern, and when the advection rate of the convection

flow is at its peak, a plume of temperature forms that forces the fluid towards the upper edge of the two types of enclosures under study. As a result, the isotherms near to the interior walls of the warmed interface in the middle of the two enclosures are warped. By adding hybrid nanofluid, it is seen that the isotherm pattern at $\varphi = 0.01$ with $Ha = 0$ was reached at $Ha = 60$ in the case without nanofluid, at $Ra = 10^6$. For this reason, we have applied the time factor. Figure 6 shows the evolution of the streamlines taking into account the time of both designed models. It is noted that using hybrid nanofluid have influence on the quick parallel arrangement of the streamlines around the gaps in the two cases.

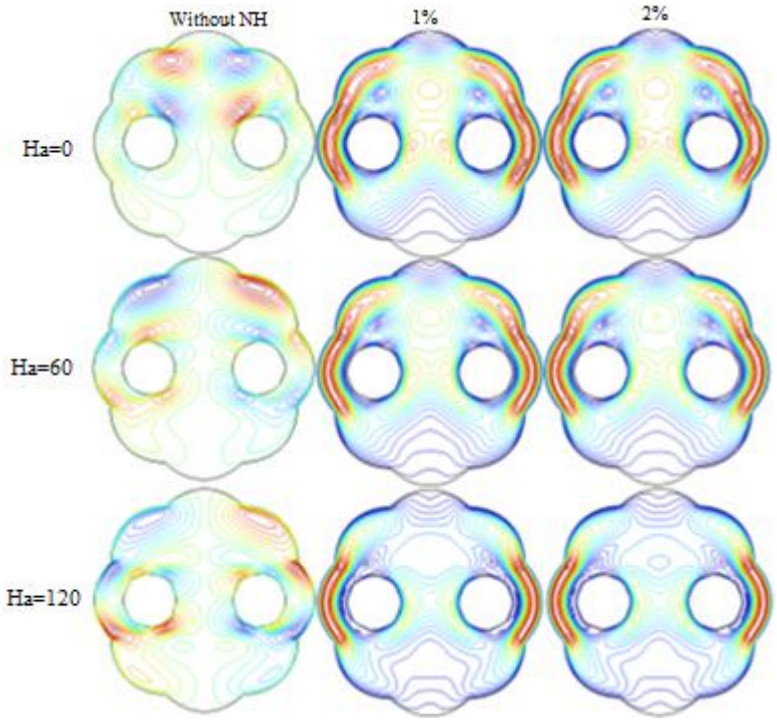

Fig. 3. Dimensionless streamlines for the flower shape at $Ra = 10^6$ in different φ values.

4.3. Heat transfer

Figure 7 shows the effect of the hybrid nanofluid's volume percentage on the Nusselt number for various Hartmann values for the two tested designs. As can be seen from the figure 7, for both the 1% and 2% volume fractions, the Nusselt number increases as the Hartmann number increases. The 2% volume fraction increases significantly more than the 1% volume fraction, with a range of 8.26% to 8.57% when considering the circular shape. Similar to the circular shape, the Nusselt number in the flower shape also increases with increasing Hartmann number for both volume fractions. The increment for the 2% volume fraction is again slightly higher than for the 1% volume fraction, ranging from 8.21% to 8.44%. Here, we see that the Nusselt number for the flower shape is consistently higher than for the circular shape at 1% volume fraction. The difference ranges from 6.34% to 7.91%. According to the 1% volume fraction scenario, the Nusselt number for the flower shape is consistently higher than that of the circular shape at 2% volume fraction. The percentage difference is between 6.35% and 7.81%. In conclusion, for both 1% and 2% volume fractions, the flower shape consistently exhibits a 6.34% to 7.91% higher Nusselt number compared to the circular shape. Additionally, the flower shape consistently exhibits a higher Nusselt number compared to the circular shape for both

volume fractions. In both scenarios, the Nusselt number reaches its greater value at $\varphi = 2\%$. Additionally, it is seen that for the same volume percent of the hybrid nanofluid, the flower shape results lead to a higher Nusselt value than the circular shape. Otherwise, the Nusselt value decreases as the Hartmann number rises in magnitude.

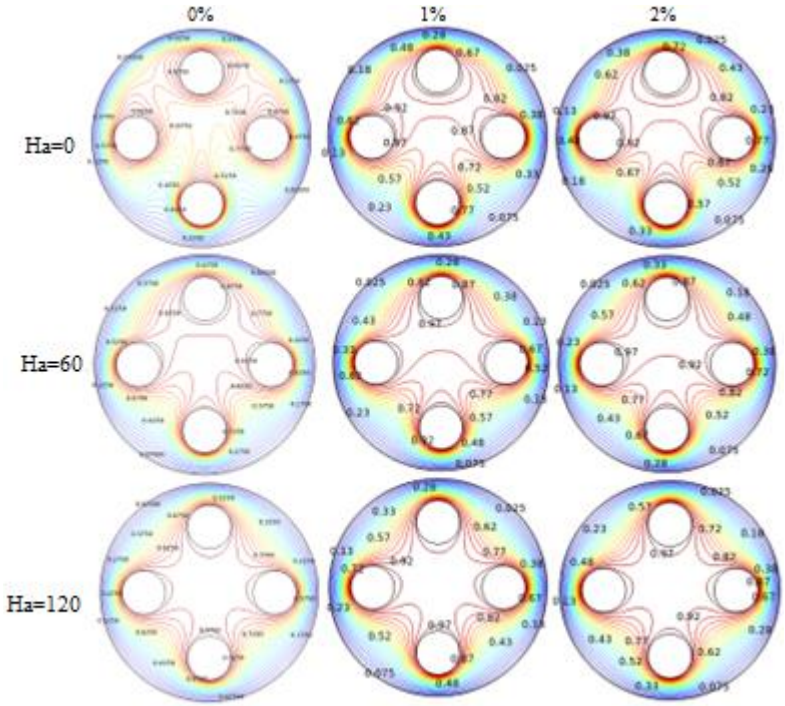

Fig. 4. Isotherms for the circular shape at $Ra = 10^6$ in different φ values.

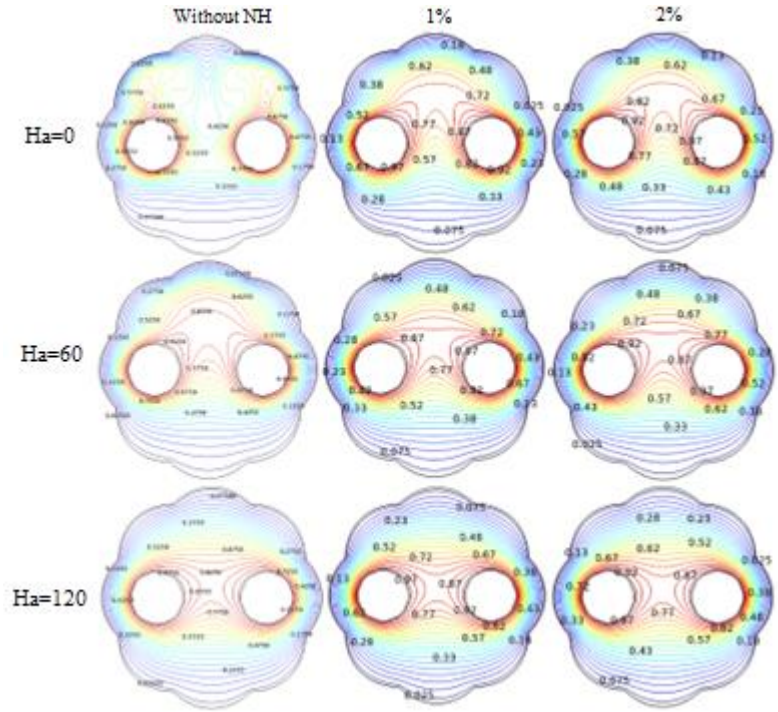

Fig. 5. Isotherms for the flower shape at $Ra = 10^6$ in different φ values.

This study breaks new ground in heat transfer by employing nanohybrids (mixtures of multiple fluids) within enclosures of varying shapes (circular and wavy) compared to existing research that focuses on nanofluids in square geometries[15,29,30]. Combining unique nanohybrids, which significantly impact thermal properties and flow patterns, with investigations of circular and wavy enclosures, this research offers fresh perspectives on optimizing heat transfer through its influence on both fluid properties and enclosure geometry. Our approach complements existing studies by analyzing similar factors like the Rayleigh and Hartmann numbers, but with the key distinction of using nanohybrids. This allows for a direct comparison of how these fluids influence flow patterns and heat transfer (through Nusselt number) compared to traditional nanofluids. Ultimately, this comparative analysis validates the potential of nanohybrids for enhanced heat transfer across different geometries, including the introduction of a novel wavy enclosure for further exploration.

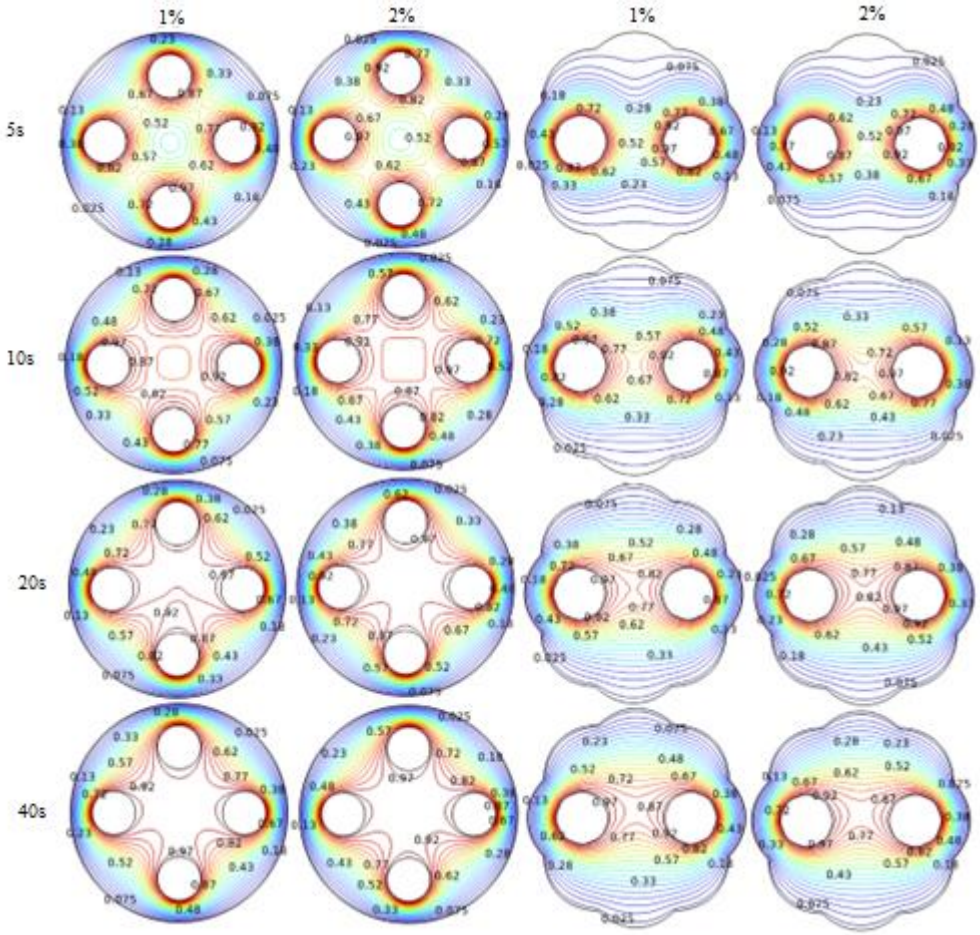

Fig. 6. Isotherms depending on time for the circular and the flower shape at $Ra = 10^6$ in different φ values.

5. Conclusion

The current study concentrates on a numerical modeling of two-dimensional mass and heat transfer of natural convection with the addition of hybrid nanofluid in the presence of a magnetic field in two separate developed models. The program Comsol Multiphysics was used to do the numerical resolution. Following the verification of our model, the effect of the nanoparticle volume fraction on the two investigated forms was demonstrated in terms of streamlines, isotherms, and Nusselt number.

The findings show that the presence of a magnetic field causes a slight attenuation of the streamline vortices inside the enclosure, and that the strength of the circulation increases with increasing Rayleigh number and reduces with increasing Hartmann numbers. However, when the volume fraction of nanoparticles rises, the effect of adding nanoparticles becomes more and more noticeable in both the examined geometries. and if you factor in time, using hybrid nanofluid can get the same outcome faster. Additionally, results show that the Nusselt number increases when the hybrid nanofluid's volume fraction is raised from 1% ($\varphi = 0.01$) to 2% ($\varphi = 0.02$). This finding reveals a possible link between volume fraction and heat transfer enhancement, which calls for additional exploration with a broader range of volume fractions. In this investigation, the design of the flower produced some significant differences in heat transfer values compared to the circular one. Additionally, incorporating hybrid nanofluids further improved heat transfer, with a noticeable effect even at a modest volume fraction increase from 1% to 2%. These findings suggest that optimizing cavity design and employing hybrid nanofluids are promising strategies for improving heat exchanger performance. In conclusion, this research on natural convection heat transfer with nanohybrids and complex geometries has the potential to significantly advance the field. By employing nanohybrids, a more intricate mixture of fluids, and exploring geometries beyond the typical square enclosure (circular and wavy shapes), our research explores unexplored areas. Future research directions could involve exploring a wider range of nanofluid volume fractions, investigating different nanoparticle combinations, and incorporating transient simulations to analyze the time-dependent behavior of heat transfer in these geometries.

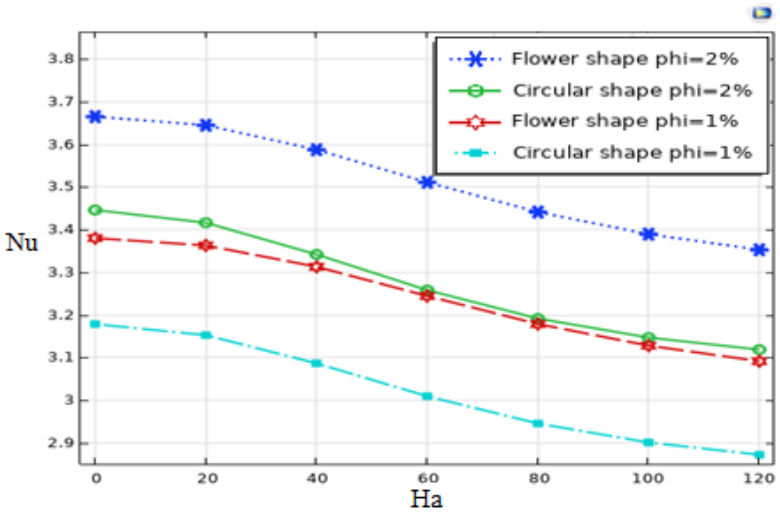

Fig. 7. Nusselt number for circular and flower shape at $Ra = 10^6$ in different φ values.

Nomenclature

Cp - Specific heat ($Jkg^{-1}K^{-1}$)
B_0 – Strength of magnetic field
k – Thermal conductivity ($Wm^{-2}K^{-1}$)
d_1 – Diameter of the inner flower shape (m)
d_2 – Diameter of the inner flower shape (m)
Nu – Nusselt number
Pr - Prandtl number
T – Temperature (K)
T_h - Temperature of hot fluid (K)
L – Diameter of the circular shape (m)
L_1 – diameter 1 of the flower shape (m)
L_2 – diameter 2 of the flower shape (m)
d – diameter of the inner cylinder (m)
Ha – Hartmann number
Ra - Rayleigh number
T* - Dimensionless temperature
T_c - Temperature of cold fluid (K)

Subscripts

hnf - Hybrid nanofluid
np – Nanoparticle

Bf – Base fluid
u, v, - Velocity components in x, and y directions
u^*, v^*, - Dimensionless velocity components
x, y, - Cartesian coordinates
x^*, y^*, - Dimensionless coordinates
Dimensionless coordinates
NH – Hybrid nanofluid
c - cold
h – hot

Greek symbols

ρ - Density (Kgm^{-3})
β - Expansion coefficient (K^{-1})
α - Thermal diffusivity (m^2s^{-1})
ϑ – Cinematic viscosity (m^2s^{-1})
μ – Dynamic viscosity ($kgm^{-1}s^{-1}$)
k_{hnf} - Thermal conductivity of the hybrid nanofluid ($Wm^{-1}K^{-1}$)
ρ_{hnf} - Density of the hybrid nanofluid (Kgm^{-3})
μ_{hnf} - Dynamic viscosity of the hybrid nanofluid ($Kgm^{-1}s^{-1}$)
$(\rho Cp)_{hnf}$ - Heat capacity of the hybrid nanofluid
φ – Volume fraction of hybrid nanofluid
ω – Direction of magnetic field, °
σ – Direction of magnetic field, (AmV^{-1})

References

[1] Ben Hamida, M.B., Hatami, M., Optimization of Fins Arrangements for the Square Light Emitting Diode (LED) Cooling through Nanofluid-Filled Microchannel, *Sci Rep, 11* (2021), pp. 12610

[2] Xu, Z., Heat Transfer Performance of the Rectangular Heat Sinks with Non-Uniform Height Thermosyphons for High Power LED Lamps Cooling, *Case Studies in Thermal Engineering, 25* (2021), pp. 101013

[3] Ben Hamida, M.B., *et al.*, A Three-Dimensional Thermal Analysis for Cooling a Square Light Emitting Diode by Multiwalled Carbon Nanotube-Nanofluid-Filled in a Rectangular Microchannel, *Advances in Mechanical Engineering 13*, (2021), 11, p. 168781402110599

[4] Chen, X., *et al.*, A Three-Dimensional Wire-Feeding Model for Heat and Metal Transfer, Fluid Flow, and Bead Shape in Wire Plasma Arc Additive Manufacturing, *J Manuf Process, 83* (2022), pp. 300–312

[5] Ferjani, B., Ben Hamida, M.B., Thermal Study of the Atomic Ratio Effect on a Cylindrical and an Ellipsoidal Shaped HgTlI Discharge Lamp, *The European Physical Journal D, 73* (2019), pp. 1-10

[6] Mahian, O., *et al.*, Performance Analysis of a Minichannel-Based Solar Collector Using Different Nanofluids, *Energy Convers Manag, 88* (2014), pp. 129–138

[7] Ben Hamida, M.B., Numerical Analysis of Tubular Solar Still with Rectangular and Cylindrical Troughs for Water Production Under Vacuum, *Journal of Taibah University for Science, 17* (2023), pp. 2159172

[8] Azzouz, R., Ben Hamida, M.B., Natural Convection in a Circular Enclosure with Four Cylinders under Magnetic Field: Application to Heat Exchanger, *Processes, 11* (2023), pp. 2444

[9] Saeidi, R., *et al.*, The Novel designs for Increasing Heat Transfer in Ground Heat Exchangers to Improve Geothermal Heat Pump Efficiency, *Geothermics, 116* (2024), pp. 102844.

[10] Purandare, P., *et al.*, Experimental Investigation on Heat Transfer and Pressure Drop of Conical Coil Heat Exchanger, *Thermal Science, 20* (2016), pp. 2087–2099

[11] Suresh, M., Mani, A., Heat and Mass Transfer Studies on a Compact Bubble Absorber in R134a-DMF Solution-Based Vapour Absorption Refrigeration System, *International Journal of Refrigeration, 36* (2013), pp. 1004–1014

[12] Ben Hamida, M.B., *et al.*, Numerical Study of Heat and Mass Transfer Enhancement for Bubble Absorption Process of Ammonia-Water Mixture without and with Nanofluids, *Thermal Science, 22* (2018), pp. 3107–3120.

[13] Yin, Y., *et al.*, Experimental Investigation of Evaporative Condensed Refrigerating System by Variation of Heat Transfer Tube Types, *Procedia Eng, 205* (2017), pp. 175–182

[14] Parvin, S., Akter, A., Effect of Magnetic Field on Natural Convection flow in a Prism Shaped Cavity Filled with Nanofluid, *Procedia Eng, 194* (2017), pp. 421–427

[15] Ben Hamida, M.B., Charrada, K., Natural Convection Heat Transfer in an Enclosure Filled with an Ethylene Glycol - Copper Nanofluid under Magnetic Fields, *Numeri Heat Transf A Appl, 67* (2015), pp. 902–920

[16] Pal, G.C., *et al.*, Natural Convection in an Enclosure with a Pair of Cylinders under Magnetic Field, *Case Studies in Thermal Engineering, 30* (2022), pp. 101763

[17] Ghasemi, B., *et al.*, Magnetic Field Effect on Natural Convection in a Nanofluid-Filled Square Enclosure, *International Journal of Thermal Sciences, 50* (2011), pp. 1748–1756

[18] Heidary, H., *et al.*, Magnetic Field Effect on Convective Heat Transfer in Corrugated Flow Channel, *Thermal Science, 21* (2017), pp. 2105–2115
[19] Ben Hamida, M.B., *et al.*, Heat and Mass Transfer Enhancement for Falling Film Absorption Process in Vertical Plate Absorber by Adding Copper Nanoparticles, *Arab J Sci Eng, 43* (2018), pp. 4991–5001
[20] Ben Jaballah, R., *et al.*, Enhancement of the Performance of Bubble Absorber using Hybrid Nanofluid as a Cooled Absorption System, *Int J Numer Methods Heat Fluid Flow, 29* (2019), pp. 3857–3871
[21] Ben Jaballah, R., *et al.*, The Influence of Hybrid Nanofluid and Coolant Flow Direction on Bubble Mode Absorption Improvement, *in: Math Methods Appl Sci, John Wiley and Sons Ltd*, (2020).
[22] Safaei, M.R., *et al.*, The Investigation of Thermal Radiation and Free Convection Heat Transfer Mechanisms of Nanofluid Inside a Shallow Cavity by Lattice Boltzmann Method, *Physica A: Statistical Mechanics and Its Applications, 509* (2018), pp. 515–535
[23] Ben Hamida, M.B., Hatami, M., Investigation of Heated Fins Geometries on the Heat Transfer of a Channel Filled by Hybrid Nanofluids under the Electric Field, *Case Studies in Thermal Engineering, 28* (2021), pp. 101450
[24] Ho, C.J., *et al.*, Preparation and Properties of Hybrid Water-Based Suspension of Al2O3 Nanoparticles and MEPCM Particles as Functional Forced Convection Fluid, *International Communications in Heat and Mass Transfer, 37* (2010), pp. 490–494
[25] Maxwell, J.C., *A Treatise of Electricity and Magnetism*., Clarendon Press, Oxford, 1873.
[26] Brinkman, H.C., *The Viscosity of Concentrated Suspensions and Solutions*, J Chem Phys, 20 (1952)
[27] Massoudi, M.D., Ben Hamida, M.B., Free Convection and Thermal Radiation of a Nanofluid Inside an Inclined L-Shaped Microelectronic Module under the Lorentz Forces' Impact, *Heat Transfer, 50* (2021), pp. 2849–2873
[28] Mehryan, S.A.M., *et al.*, Numerical Study on Natural Convection of Ag–MgO Hybrid/Water Nanofluid Inside a Porous Enclosure: A Local Thermal Non-Equilibrium Model, *Powder Technol, 367* (2020), pp. 443–455
[29] Khanafer, K., *et al.*, Buoyancy-driven heat transfer enhancement in a two-dimensional enclosure utilizing nanofluids, Int J Heat Mass Transf, 46 (2003), pp. 3639–3653
[30] Sheikholeslami, M., *et al.*, Magnetic Field Effects on Natural Convection Around a Horizontal Circular Cylinder Inside a Square Enclosure Filled with Wanofluid, *International Communications in Heat and Mass Transfer, 39* (2012), pp. 978–986

Paper submitted: 09.01.2024.
Paper revised: 19.04.2024
Paper accepted: 24.04.2024.